4-4-2019

Reactions at Noble Metal Contacts with Methylammonium Lead Triiodide Perovskites: Role of Underpotential Deposition and Electrochemistry

Ross A. Kerner
Princeton University

Philip Schulz
National Renewable Energy Laboratory; Institut Photovoltaïque d'Ile de France (IPVF)

Jeffrey A. Christians
National Renewable Energy Laboratory; Hope College, christians@hope.edu

Sean P. Dunfield
National Renewable Energy Laboratory; University of Colorado Boulder

Benjia Dou
National Renewable Energy Laboratory; University of Colorado Boulder

Follow this and additional works at: https://digitalcommons.hope.edu/faculty_publications

Part of the Chemical Engineering Commons
See next page for additional authors

Recommended Citation

Authors

Ross A. Kerner, Philip Schulz, Jeffrey A. Christians, Sean P. Dunfield, Benjia Dou, Lianfeng Zhao, Glenn Teeter, Joseph J. Berry, and Barry P. Rand

Reactions at noble metal contacts with methylammonium lead triiodide perovskites: Role of underpotential deposition and electrochemistry

Ross A. Kerner [iD], Philip Schulz [iD], Jeffrey A. Christians [iD], Sean P. Dunfield [iD], Benjia Dou [iD], Lianfeng Zhao [iD], Glenn Teeter [iD], Joseph J. Berry [iD], and Barry P. Rand [iD]

COLLECTIONS

Paper published as part of the special topic on Perovskite Semiconductors for Next Generation Optoelectronic Applications

View Online   Export Citation   CrossMark

ARTICLES YOU MAY BE INTERESTED IN

Verification and mitigation of ion migration in perovskite solar cells
APL Materials **7**, 041111 (2019); https://doi.org/10.1063/1.5085643

Unusual defect physics in $CH_3NH_3PbI_3$ perovskite solar cell absorber
Applied Physics Letters **104**, 063903 (2014); https://doi.org/10.1063/1.4864778

Water in hybrid perovskites: Bulk $MAPbI_3$ degradation via super-hydrous state
APL Materials **7**, 041112 (2019); https://doi.org/10.1063/1.5087290

Reactions at noble metal contacts with methylammonium lead triiodide perovskites: Role of underpotential deposition and electrochemistry

Ross A. Kerner,[1] (ID) Philip Schulz,[2,3] (ID) Jeffrey A. Christians,[2,4] (ID) Sean P. Dunfield,[2,5,6] (ID) Benjia Dou,[2,7] (ID) Lianfeng Zhao,[1] (ID) Glenn Teeter,[2] (ID) Joseph J. Berry,[2] (ID) and Barry P. Rand[1,8] (ID)

AFFILIATIONS

[1] Department of Electrical Engineering, Princeton University, Princeton, New Jersey 08544, USA
[2] National Renewable Energy Laboratory, Golden, Colorado 80401, USA
[3] CNRS, Institut Photovoltaïque d'Ile de France (IPVF), UMR 9006 Palaiseau, France
[4] Department of Engineering, Hope College, Holland, Michigan 49423, USA
[5] Materials Science and Engineering Program, University of Colorado Boulder, Boulder, Colorado 80309, USA
[6] Renewable and Sustainable Energy Institute, University of Colorado Boulder, Boulder, Colorado 80309, USA
[7] Department of Electrical, Computer, and Energy Engineering, University of Colorado Boulder, Boulder, Colorado 80309, USA
[8] Andlinger Center for Energy and the Environment, Princeton University, Princeton, New Jersey 08544, USA

Note: This paper is part of the special topic on Perovskite Semiconductors for Next Generation Optoelectronic Applications.

ABSTRACT

Chemical reactivity of halide perovskites coupled with a low energy of formation makes it a challenge to characterize material properties and achieve long-term device stability. In this study, we elucidate electrochemical reactions occurring at the methylammonium lead triiodide ($MAPbI_3$)/Au interface. X-ray photoemission spectroscopy is used to identify a type of reduction/oxidation reaction termed underpotential deposition (UPD) involving lead, iodine, and hydrogen occurring at interfaces with noble metals. Changes in surface compositions and oxidation states suggest that UPD derived adsorbates at $MAPbI_3$/Au interfaces lower the energy barrier for release of volatile HI and/or I_2 catalyzing degradation at exposed contacts. Additionally, comparison to PbI_2/Au interfaces demonstrates that the presence of methylammonium/methylamine accelerates the formation of a Pb^0 adlayer on the Au. Reactions involving UPD Pb^0 can transform the typically anodic (hole collecting) Au to a cathode in a photovoltaic measurement. Cyclic voltammetry reveals electrochemical reaction peaks in indium tin oxide (ITO)/$MAPbI_3$/Au devices occurring within voltage ranges commonly used for perovskite characterization. The electrochemical stability window of this device architecture is measured to be between −0.5 V and 0.9 V. Voltage induced interfacial reactions contribute to reversible electrochemical peaks, hysteresis, switchable perovskite diode polarity, and permanent degradation at larger voltages. These types of surface reactions alter the interface/interphase composition beyond ion accumulation, provide a source for the diffusion of defects, and contribute to electrode material dependent current-voltage hysteresis. Moreover, the results imply fundamental limitations to achieving high device stability with noble metals and/or methylammonium containing perovskites.

Metal halide perovskite materials have been successfully employed as the active layer in numerous types of optoelectronic devices.[1–4] While this class of materials displays many attractive qualities for a semiconductor such as ease of processing and tunable bandgap across the ultraviolet/visible/near-infrared spectral range, there are many challenges to be overcome prior to

commercialization. Currently, the most important challenge is predicting with high certainty long-term device stability for various applications.[5,6] Instability of the prototypical methylammonium containing lead (Pb) halide perovskites is an intrinsic problem dictated by fundamental thermodynamics and was one of the earliest concerns expressed about the prospective of these materials for photovoltaics.[7] This is because methylammonium halide perovskites have relatively low (but favorable) or even unfavorable energies of formation. While low formation energies allow, for example, low temperature solution processing,[8] it also implies that the material will be prone to chemical transformations under minimal external energy input.

Due to an assumed inertness, noble metals such as Au are commonly used as electrodes for perovskite devices. Direct perovskite/Au interfaces are often found in halide perovskite based diodes displaying switchable polarity, memristive devices, field-effect transistors, Hall effect samples, space charge limited current (SCLC) measurements, time of flight measurements, and when Au is used as a conductive substrate for photoemission spectroscopy.[9–13] Lateral devices composed of noble metal electrodes bridged by methylammonium lead triiodide (MAPbI$_3$) or methylammonium lead tribromide (MAPbBr$_3$) rapidly degrade to PbI$_2$ and PbBr$_2$, respectively, upon voltage bias.[14–17] These results clearly illustrate electrochemical activity at noble metal/perovskite interfaces under large voltage bias and support the mechanism of H$_2$ and I$_2$ generation at the cathode and anode, respectively, proposed by Frolova *et al.*[17] Even when a buffer layer physically separates the perovskite from the noble metal, as is common in devices, direct perovskite/Au contact is unavoidable at pinhole defects in these layer stacks, such as with the prototypical organic hole transport material 2,2′,7,7′-tetrakis(*N,N*-di-*p*-methoxyphenylamino)-9,9′-spirobifluorene (Spiro-OMeTAD) which is notorious for a high density of pinholes.[18] Electrochemical reactions at these defects may contribute to long term degradation of perovskite devices and efficiency loss mechanisms attributed to device interfaces.[5,6,18,19]

It is also possible that noble metals can be incorporated into the halide perovskite lattice, reacting to form materials such as CsAuI$_4$ and MA$_2$Au$_2$I$_6$.[20–22] However, the conditions for forming such noble-metal-containing perovskites are relatively extreme and have not yet been confirmed to form under typical perovskite device operating conditions. Lesser known underpotential deposition (UPD) reactions, a form of surface-limited reduction/oxidation reactions, are also known to occur with many ions at noble metal electrodes near the equilibrium potential.[23] Underpotential deposition is a type of surface adsorption reaction in which an ion changes oxidation state upon adsorption. These reactions occur spontaneously at voltages lower than the bulk reaction potential. For example, a partial monolayer of reduced Pb spontaneously adsorbs to Au at 0 V (relative to Ag/AgCl electrode) whereas bulk Pb^0 electrodeposition does not occur until −0.25 V.[24] A positive voltage of 0.15 V must be applied to strip this monolayer of UPD Pb desorbing as Pb^{2+}.[24] Furthermore, the adlayer structure rearranges as a function of voltage, counterion, and organic additives.[23] Nearly all relevant halide perovskite components including H$^+$, Cs$^+$, Pb^{2+}, and halide anions are known to participate in UPD reactions.[23–28] While permanent electrochemical degradation can be avoided by operating at low voltages within an electrochemically stable window,

UPD reactions remain active at low voltages and can substantially affect the structure and properties of an interface, or what might be more helpful if referred to as an interphase when discussing a metal/solid electrolyte.[29] Interphases and UPD reactions within perovskite devices have potentially significant implications with regard to current-voltage hysteresis and long-term degradation pathways.

In this work, we identify the formation of UPD Pb and I species at direct MAPbI$_3$/Au contacts. Our results indicate that the MAPbI$_3$/Au interface catalyzes HI formation and loss of methylammonium iodide (MAI) accelerating degradation of MAPbI$_3$ to PbI$_2$. The formation of UPD species is affected by the chemical environment which we observe during X-ray photoemission spectroscopy (XPS) leading to a rapid *in situ* deposition of Pb^0 on the Au surface when in contact with MAPbI$_3$ but not for the PbI$_2$/Au interface. Comparison to PbI$_2$/Au heterojunctions allows us to outline reaction mechanisms and elucidate the direct involvement of the organic methylammonium/methylamine molecule in the Pb^0 reaction pathway presumably involving proton transfer reactions. Photovoltage measured by XPS reveals that this reaction causes the MAPbI$_3$/Au contact, which is typically anodic, to become a cathode. These results reveal how a subtle reaction can have a significant effect on the interface composition, diode properties/polarity, material stability, and possible artifacts in XPS measurements. Additionally, the implications of this work elucidate possible limitations of noble metals and methylammonium containing perovskites for long term operation of halide perovskite-based optoelectronic devices.

Details of MAPbI$_3$ and PbI$_2$ film deposition can be found in the supplementary material. Most importantly, the fabrication process employed here produces smooth, small grained MAPbI$_3$ and PbI$_2$ films with root-mean-square (RMS) roughnesses of approximately 4 nm and 6 nm, respectively. This work is organized into three main sections. First, we examine PbI$_2$ and MAPbI$_3$ films coated with thick Au to confirm the existence of UPD adsorbates via XPS binding energy (BE) signatures and further show differences in formation kinetics in the presence (MAPbI$_3$) and absence (PbI$_2$) of protons which are undetectable by XPS. Second, after establishing the presence of UPD species, samples coated with thin Au films (5 nm) are characterized to elucidate reactions occurring at the buried PbI$_2$/Au and MAPbI$_3$/Au interfaces. Only in the case of MAPbI$_3$/Au do we observe rapid formation of a self-limiting amount of Pb^0, suggesting protons and/or methylamine influences the formation kinetics and oxidation state of UPD layers on the Au. Third, we perform cyclic current density-voltage (*J-V*) measurements of indium tin oxide (ITO)/MAPbI$_3$/Au devices displaying electrochemical features which support the plausibility that interface reactions occur within normal operating voltages (<1 V) of common perovskite-based devices.

Sequential XPS measurements of MAPbI$_3$ and PbI$_2$ covered with thick (50 nm) Au films are displayed in Fig. 1. Despite Au thicknesses well above the escape depth of photoelectrons (<10 nm), Pb and iodine species are still detected in sizeable amounts (see Tables S1 and S2 for relative atomic ratios). This suggests that Pb and iodine are present on the Au top surface (see Figs. S1–S3 for more evidence that the Au layers are neither discontinuous nor transparent to photoelectrons). These elements likely accumulate on the Au by surface diffusion during thermal deposition of Au. We assume that initial deposition forms islands of Au, each coated in a partial
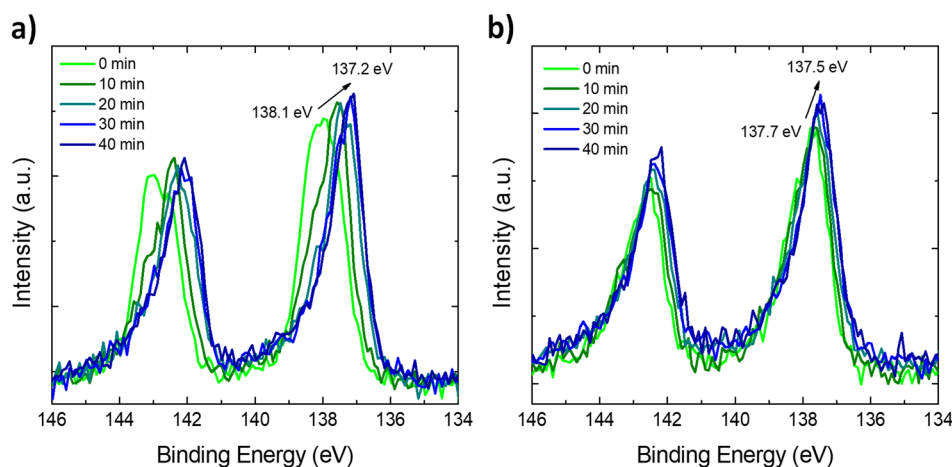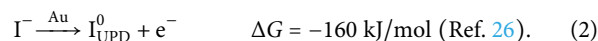
FIG. 1. Consecutive XPS measurements of the Pb 4f region of (a) $MAPbI_3$ and (b) PbI_2 coated with thick (50 nm) Au films.

monolayer of adsorbates, which eventually coalesce to form a contiguous film of Au. Further Au deposition builds to the bulk Au thickness, while the adsorbates (only covering a fraction of the surface, Table S2) can remain on the surface instead of incorporating into the Au bulk. Alternatively, adsorbates may diffuse along surfaces and grain boundaries through the Au film. Continuous XPS measurements reveal that the Pb $4f_{7/2}$ peak gradually shifts from BE near 138.1 eV to BE $\approx$ 137.2 eV and 137.7 eV to 137.5 eV for $MAPbI_3$/Au and PbI_2/Au, respectively, indicating a change in chemical bonding environment. Note that these samples were grounded to both the ITO and Au simultaneously. The Au $4f_{7/2}$ peaks were stable and located at the expected BE of 84.1 eV (Fig. S4) for the duration of the XPS measurements in Fig. 1. The Pb $4f_{7/2}$ BE at approximately 137.5 eV correlates to neither Pb^{2+} (BE $\geq$ 138 eV) nor Pb^0 (BE < 137 eV). However, this BE is consistent with reported BEs of UPD Pb (denoted Pb_{UPD}) on Au (~137.4 eV).[24,30] It appears that some of this new Pb species has already formed in the initial scan for PbI_2/Au, whereas it takes some energy input to form this species in $MAPbI_3$/Au.

Further insight into chemical alterations at this surface is gained from XPS measurements of the I 3d region of the samples covered by 50 nm of Au as displayed in Fig. 2. Binding energies for UPD iodine (denoted I^0_{UPD}) are reported to be slightly lower than iodide (618.4 eV for I^0_{UPD} vs 618.7-619.6 eV for iodide anions).[31] Measurements of iodine adsorbed on Au exposed to gaseous I_2 displayed an I $3d_{5/2}$ BE = 618.5 eV in close agreement to I^0_{UPD}, but the simultaneous presence of Pb atoms in the samples in Fig. 2 may also influence the BE making I^0_{UPD} difficult to unambiguously identify. The initial I 3d spectra for both $MAPbI_3$/Au and PbI_2/Au samples look very similar; however, their degradation characteristics differ significantly. Figure 2(a) reveals that reactions at the $MAPbI_3$/Au interface induced by X-ray irradiation result in a rapid and significant loss of iodine over time with no significant change in the oxidation state (see Table S2 for relative atomic ratio changes). By contrast, the PbI_2/Au sample in Fig. 2(b) displays a slight increase in the iodine signal evidenced by the emergence of a high BE feature at approximately 620.5 eV. This BE corresponds to molecular iodine, or, more likely, a triiodide species bonded to the surface. These prominent differences in degradation behavior

between $MAPbI_3$/Au and PbI_2/Au suggest differing reaction mechanisms. The $MAPbI_3$/Au iodide loss is likely in the form of volatile HI. On the other hand, the absence of protons in PbI_2 precludes HI formation. The remaining possibility is that iodine leaves as I_2 which, due to its relatively low volatility, accumulates on the surface as triiodide leading to an increase in the intensity of the feature centered at 620.5 eV in Fig. 2(b). Signals from oxygen and nitrogen are extremely low for these samples, and the C 1s peak remains unchanged during X-ray irradiation which rules out surface contaminants as the source of the observed changes in oxidation states (Fig. S5). The primary reactants at the top Au surface are limited to Pb, iodine, and H^+.

Underpotential deposition reactions are well characterized for both Pb and iodide on Au surfaces and shown, respectively, by reaction Eqs. (1) and (2)

$$Pb^{2+} \xrightarrow{Au} Pb_{UPD}, \tag{1}$$

$$I^- \xrightarrow{Au} I^0_{UPD} + e^- \qquad \Delta G = -160 \text{ kJ/mol (Ref. 26).} \tag{2}$$

The XPS BE of Pb $4f_{7/2} \approx$ 137.5 eV in Fig. 1 suggests that these surface species are forming at solid-state interfaces between PbI_2/Au and $MAPbI_3$/Au as well. Note that the chemical state of UPD adsorbed species can differ from that of the bulk or elemental material despite having the same oxidation state. For example, reaction 2 is posited to result in the spontaneous adsorption of neutral atomic iodine (as opposed to molecular iodine).[26,31] Because of this, the measured BE of I^0_{UPD} is more similar to an iodide anion than for molecular iodine.[31] It is not well established what the oxidation state of Pb_{UPD} is (i.e., whether it is partially or wholly reduced) and, thus, the number of electrons is omitted in Eq. (1).[24,30] As will be shown, our XPS data suggest Pb_{UPD} can adsorb in at least two different chemical states. Intermediate oxidation states are supported by calculations suggesting that partially reduced Pb ions can be stabilized as dimers (e.g., $[Pb_2]^{3+}$ or $[Pb_2]^{2+}$).[32] Cyclic voltammetry of Pb_{UPD} on Au (110) surfaces displays three peaks, and the oxidation state of Pb_{UPD} may proceed through several different partial charges. Additionally, UPD reactions are well characterized for H^+.[23] In fact, the reaction potential of Eq. (2) is known to be strongly pH dependent
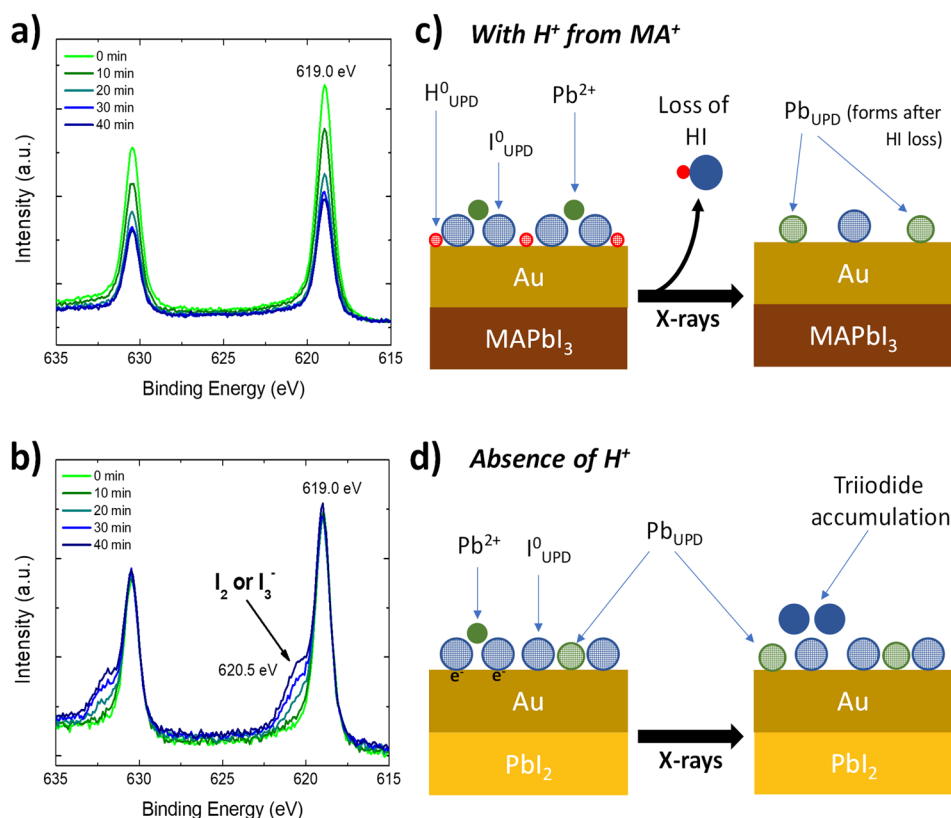
FIG. 2. Consecutive XPS measurements of the I 3d region of (a) MAPbI$_3$ and (b) PbI$_2$ coated with thick (50 nm) Au films. Schemes in (c) and (d) illustrate the evolution during XPS measurements of the UPD layer on the top Au surface for MAPbI$_3$/Au and PbI$_2$/Au, respectively. UPD adsorbed species are designated with a hashed fill.

on many metals due to both H$^0_{UPD}$ and I$^0_{UPD}$ simultaneously taking part in the adsorption/desorption reactions.[33] We hypothesize that the protons in MAPbI$_3$ interact with I$^0_{UPD}$, altering adsorption kinetics as well as facilitating evolution of different products during X-ray irradiation.

Surface reconstructions that involve changes in stoichiometry, oxidation state, arrangement of ionic layers, and chemical reactions at the MAPbI$_3$/Au boundary motivate us to adopt the term interphase as is commonly referenced in the battery community.[34] The evolution of elemental concentrations and oxidation states of Pb and iodine on the Au surface indicates that non-negligible changes in the chemical structure of the interphase are occurring during the XPS measurement. Illustrations of surface reactions and changes in the interphase structure at the top Au surface are depicted in Figs. 2(c) and 2(d) for MAPbI$_3$/Au and PbI$_2$/Au, respectively. The BE shifts of Pb 4f$_{7/2}$ in Fig. 1 is suggestive that Pb$_{UPD}$ has not fully reacted prior to X-ray irradiation. This indicates that the strongest spontaneous interaction is between iodide/Au which separates Pb^{2+} ions by a layer of I$^0_{UPD}$, as shown in the initial structures in Figs. 2(c) and 2(d). However, for PbI$_2$/Au, Fig. 1(b) leads us to assume that some Pb$_{UPD}$ has formed. Upon energy input (X-ray absorption, photoelectron collisions, etc.), I$^0_{UPD}$ undergoes further reactions or rearrangement. In the case of MAPbI$_3$ in contact with Au, abundant methylammonium provides protons which are also known to form UPD H^0 by consuming the electron released from iodide. The adsorbed H^0 delays the formation of Pb$_{UPD}$ and is presumed to react with I$^0_{UPD}$ to form volatile HI [Fig. 2(c)]. Under more device relevant

conditions, thermal degradation of MAPbI$_3$ to PbI$_2$ is accelerated at the edges of Au contacts as shown in Fig. 3 which we attribute to catalyzed HI loss by this mechanism. We cannot rule out H$_2$ and I$_2$ evolution instead of HI, but the overall effect is the same and both reaction pathways likely occur simultaneously. On the other hand, PbI$_2$ can only release iodine as molecular iodine/triiodide, as shown in Fig. 2(d). When iodide or I$^0_{UPD}$ is lost, Pb^{2+} consumes the electrons to adsorb directly to the Au as Pb$_{UPD}$ shifting to slightly lower BE (as in Fig. 1). The main difference is the presence of protons participating in the surface reactions to have non-negligible effects on the reaction rates and resulting surface composition.

Chemical changes in the buried MAPbI$_3$/Au and PbI$_2$/Au interfaces were characterized by probing a MAPbI$_3$/thin Au (nominally 5 nm) junction. Figure 4 displays the evolution of Pb 4f peaks for thin Au films coating the MAPbI$_3$ or PbI$_2$ (XPS of I 3d, N 1s, C 1s, and Au 4f is provided in Figs. S6 and S7). The MAPbI$_3$/thin Au sample [Fig. 4(a)] initially contains only Pb^{2+} (4f$_{7/2}$ BE ≈ 138.0 eV) indicating that the metal evaporation does not directly induce any Pb^0. Indeed, using tape to delaminate a 50 nm thick Au electrode revealed undamaged and stable MAPbI$_3$ below it (Fig. S8). For MAPbI$_3$/thin Au, intense X-ray irradiation induces the growth of signal from metallic Pb^0 (4f$_{7/2}$ BE ≈ 136.8 eV) over the course of 16 min of continuous X-ray exposure. Processing and morphology effects were ruled out by characterizing larger grained MAPbI$_3$/Au 5 nm where MAPbI$_3$ was processed with dimethylsulfoxide additive (1:1 molar ratio with respect to PbI$_2$) for which similar Pb^0 formation was observed. By contrast, no Pb^0 was observed to form at
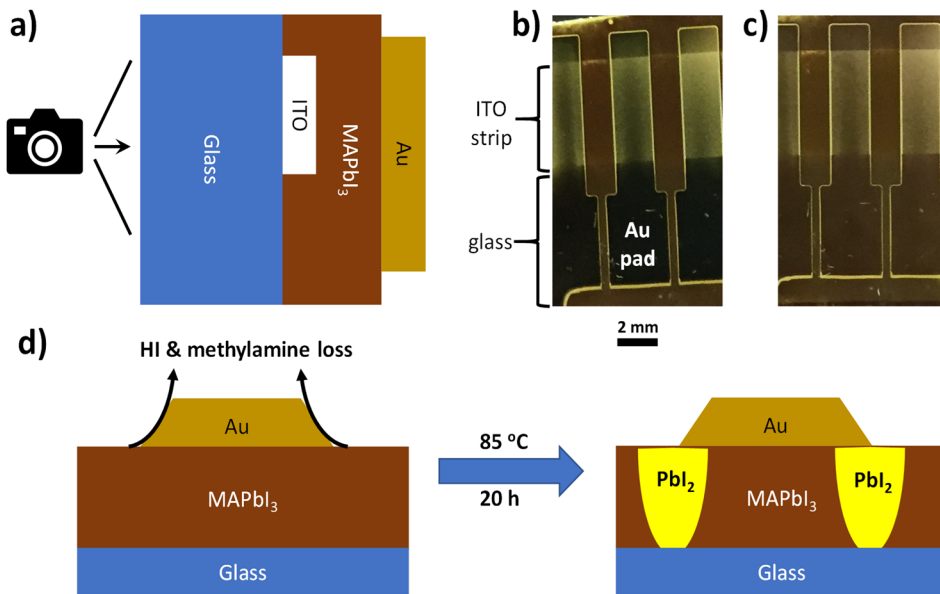
FIG. 3. Images of MAPbI$_3$ degradation at 85 °C in N$_2$ for 20 h. Photographs taken through the glass as shown in (a) of the degraded sample (b) with the Au and (c) after delaminating the Au with tape. Accelerated degradation to PbI$_2$ is observed at the edges of the Au as shown in the cartoon in (d) relative to areas of MAPbI$_3$ on ITO and glass without Au.

PbI$_2$/thin Au interfaces nor does Pb^0 develop on such short time scales for MAPbI$_3$ and PbI$_2$ control films (Fig. S9). Consistent with Fig. 2, the I 3d peak indicates an accelerated loss of iodine from MAPbI$_3$/thin Au whereas no iodine is lost from the PbI$_2$/thin Au sample (Figs. S6a and S7a).

Formation of Pb^0 at the MAPbI$_3$/Au interface was observed on a variety of substrates including ITO, ITO/SnO$_2$, fluorine doped tin oxide (FTO)/TiO$_2$, Si, and ITO/poly-TPD (poly[N,N′-bis(4-butylphenyl)-N,N′-bis(phenyl)-benzidine]) ruling out the bottom contact as a source of chemical changes (Fig. S10). Similar behavior is observed for MAPbI$_3$ and PbI$_2$ interfaced with Ag and Ir (Fig. S11) indicating the choice of noble metal is also inconsequential and correcting our earlier conclusion for perovskite/Ag reactions (i.e., Ag reacts more similarly to a noble metal than a reductive metal which reacts by direct metal/metal cation redox).[35] Note that Pb^0 formation is only observed for Au on top of MAPbI$_3$; the use of Au as a substrate did not facilitate Pb^0 formation at the top surface of MAPbI$_3$ (180 nm thickness). However, we cannot rule out Pb^0 formation or reactions at the buried Au/MAPbI$_3$ interface where we would expect the interface reaction to occur in this sample geometry. These observations clearly indicate that the organic methylammonium cation is involved in the reaction pathway that produces Pb^0. Once the methylammonium is deprotonated, methylamine is left to react with Pb^{2+}. Our recent work shows that exposing PbI$_2$ to amines leads to rapid Pb^0 formation during XPS measurements.[36] The proposed reaction pathway with an alkylamine proceeds through an initial α-N-H proton transfer reaction forming Pb-iodo-amides and a second β-C-H proton transfer reaction to ultimately produce HI, the Schiff base (imine) of the amine, and Pb^0.[36] The formation of volatile byproducts including the Schiff base, HI, and H$_2$ is strongly supported by the formation of a bubble in the Au film where X-rays were incident, as shown in Fig. S3 indicating that the reaction also occurs at the buried MAPbI$_3$/Au (50 nm) interface, simultaneously proving the completeness of the Au film. Figure S12 shows Pb 4f
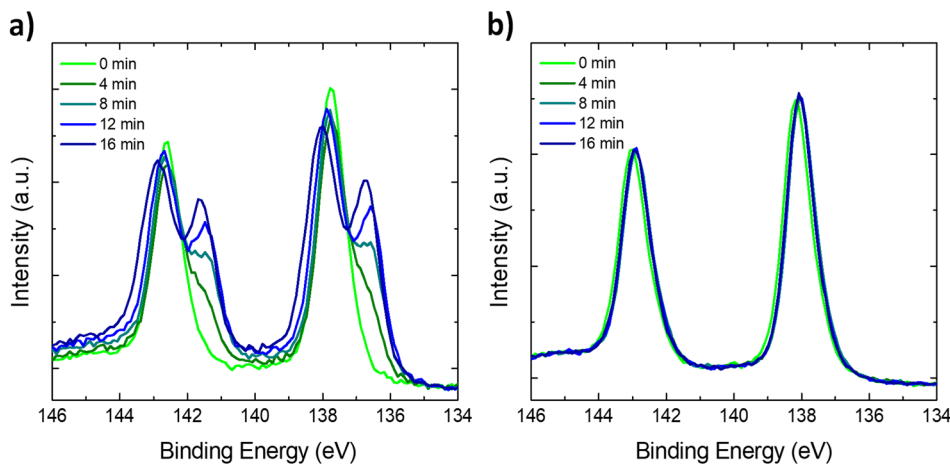

FIG. 4. Consecutive XPS measurements of the Pb 4f region of (a) MAPbI$_3$ and (b) PbI$_2$ coated with thin (5 nm) Au films.
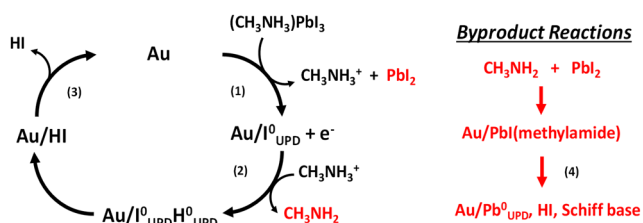
XPS of MAPbI$_3$/Au with even thinner Au (0.5 nm) as well as the MAPbI$_3$/Au (5 nm) but to longer measurement times. The amount of Pb^0 increased asymptotically, and the final amount was correlated with the amount of Au deposited. This leads us to conclude that the Pb^0 is adsorbed to the Au surface in the form of Pb$^0_{UPD}$, chemically different from the Pb$_{UPD}$ formed in Fig. 2. The reaction likely terminates once the catalytic surface of the Au is covered in Pb$^0_{UPD}$. In comparison with PbI$_2$/Au, the presence of methylammonium/methylamine at this interface modifies the oxidation state of the adsorbed Pb species that form under irradiation.

The accumulation of the above results as well as our previous work on PbI$_2$/amine reactions allows us to propose Scheme 1 for the degradation pathway of MAPbI$_3$/noble metals during XPS measurements. In the case of MAPbI$_3$/Au,

(1) Electrons are released upon the adsorption of I$^0_{UPD}$ onto Au, producing PbI$_2$ and methylammonium.
(2) A proton from methylammonium adsorbs to the Au surface, captures the free electron, and liberates methylamine.
(3) The adsorbed I$^0_{UPD}$ and H$^0_{UPD}$ then react to be released as volatile HI, I$_2$, and/or H$_2$ gases.
(4) In a subsequent reaction, the methylamine and PbI$_2$ byproducts react via proton transfer reactions and amido Pb intermediates to form more HI, volatile organic species, and Pb$^0_{UPD}$.[36]

It is reasonable that the noble metal catalyzes proton transfer reactions in step (4) as Au nanoparticles are known to catalyze dehydrogenation of organic molecules involving the β-C-H proton.[37] Less catalytic bulk Au has also been shown to catalyze hydrogen and alkyl group elimination of aliphatic amines to produce imines.[38] However, the reaction stops once the Au surface is coated in a layer of Pb$^0_{UPD}$. When the Au is Pb terminated, it no longer looks like Au and loses its ability to adsorb I$^0_{UPD}$ to catalyze HI loss. In contrast to MAPbI$_3$/Au, while PbI$_2$/Au similarly releases electrons due to the iodide UPD reaction at the Au surface, the only destination for these electrons is Pb^{2+} cations in the UPD reaction, forming Pb$_{UPD}$ and an accumulation of oxidized iodide. Both methylamine and free H$^+$ are expected to be much more mobile than Pb^{2+}, accelerating the rate of reactions in MAPbI$_3$ vs PbI$_2$ (as observed in Figs. 1 and 2). The above proposed mechanisms are consistent with the following observations:

- Identification of UPD Pb and iodine species on Au surfaces
- Rapid iodide loss in MAPbI$_3$/Au
- Triiodide accumulation in PbI$_2$/Au

- Pb^0 formation at MAPbI$_3$/noble metal interfaces
- The absence of Pb^0 formation at PbI$_2$/noble metal interfaces

The reactions producing Pb$^0_{UPD}$ at the Au interface appear to impact the electronic characteristics of diodes with Au electrodes. Direct perovskite/Au contacts are commonly regarded as an anode, but it is also known that the Au can become the cathode upon voltage bias.[9,39–42] In XPS measurements, we observe the Au to be cathodic in our ITO/MAPbI$_3$/Au (5 nm) devices. Figures 5(a) and 5(b) show the Au 4f$_{7/2}$ and valence XPS spectra of an ITO/MAPbI$_3$/Au (5 nm) sample in the dark and under illumination (the data in Fig. 5 were obtained after 20 min of X-ray irradiation followed by 60 min of resting in the analysis chamber). In the absence of visible light illumination, the Au 4f$_{7/2}$ BE is 83.8 eV, 0.2–0.3 eV lower than that of bulk Au [Fig. 5(a)]. This is accompanied by a Fermi energy shifted to −0.25 eV with respect to the Fermi energy of the instrument [Fig. 5(b)]. The 5 nm thick Au film is not continuous, and
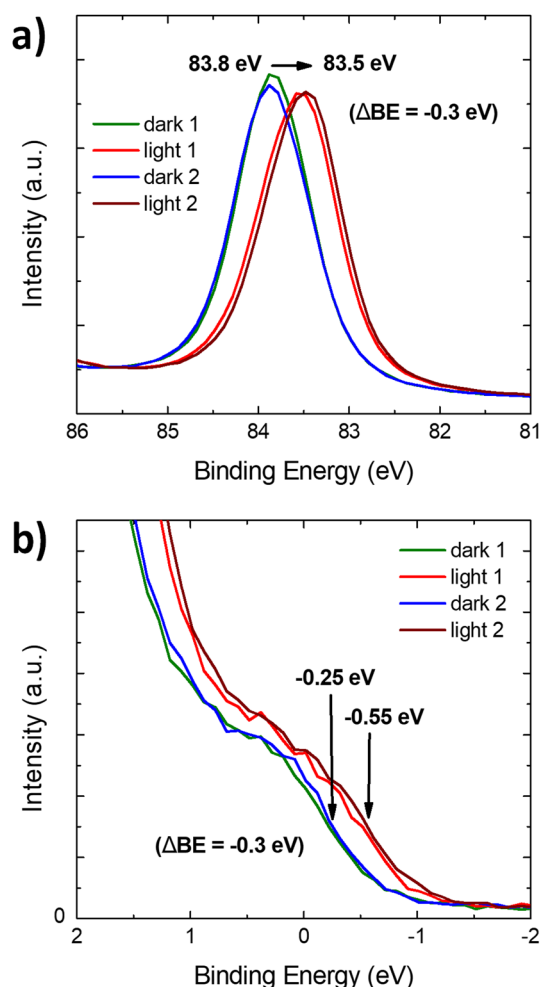
FIG. 5. XPS of the (a) Au 4f$_{7/2}$ peak and (b) valence region of an ITO (ground)/MAPbI$_3$/Au (5 nm) sample showing illumination induced photovoltage to negative voltages where the Au acts as the cathode.

SCHEME 1. Proposed noble metal catalyzed degradation at MAPbI$_3$/Au heterojunctions (Au thickness = 5 nm) observed during XPS measurements where the byproducts methylamine and PbI$_2$ (in red) lead to the eventual formation of Pb^0.

therefore, the sample is grounded only by the ITO, leaving the Au electronically floating. Negative BE shifts in Fig. 5 mean that there is a −0.25 V electrical bias between the Au and the grounded ITO. We attribute this voltage difference to electron accumulation at the Au and resulting photovoltage produced by excitations from X-ray absorption and photoelectron collisions within the bulk of the MAPbI$_3$ layer. Photovoltage sourcing these negative BE shifts is confirmed by reversible shifts to lower energy when illuminated by the XPS analysis chamber lights. Measured shifts under visible light illumination are ΔBE ≈ −0.3 eV for both the Au 4f$_{7/2}$ peak and Au Fermi energy to 83.5 eV and −0.55 eV, respectively. Further evidence confirming X-ray induced photovoltage is provided by positive BE shifts of a FTO/MAPbI$_3$/poly-TPD (40 nm)/Au (0.5 nm) device shown in Fig. S13. The insertion of the hole transporting polymer between the MAPbI$_3$ and Au ensures that the poly-TPD/Au contact is the anode, reversing the direction of the photovoltage and BE shifts measured by XPS.

The magnitude of the cathodic Au photovoltage is also observed to change over time as the interface reaction progresses. For samples with direct ITO/MAPbI$_3$ contact, the photovoltage often decreases at long times as in Fig. S6d. We attribute this to a minor but a detrimental reaction or ion accumulation at the ITO/MAPbI$_3$ interface that increases the non-radiative recombination rate (hence, the choice of FTO for the device in Fig. S13). By contrast, for samples avoiding direct contact between ITO and MAPbI$_3$, the photovoltage monotonically increases to a stable value. Figures S14 and S15 show the XPS evolution of the Fermi edge and Au 4f$_{7/2}$ peak for ITO/poly-TPD (40 nm)/MAPbI$_3$/Au (5 nm) and FTO/TiO$_2$/MAPbI$_3$/Au (5 nm) samples, respectively, as a function of time. The increase in the magnitude of the photovoltage occurs simultaneously with the growth of the Pb^0 peak during consecutive XPS scans. Eliminating the quenching ITO/MAPbI$_3$ interface by insertion of poly-TPD increases the maximum photovoltage to −0.8 V (−0.9 V with additional visible light illumination). The cathodic behavior of Au in the FTO/TiO$_2$/MAPbI$_3$/Au device is somewhat counterintuitive since TiO$_2$ is known to be a good electron collecting layer. Overall, the observation of a dynamically shifting negative voltage concomitant with chemical changes means the electronic properties of a MAPbI$_3$/Au interface can be changed quite drastically as a result of *in situ* UPD reactions and interphase reconstructions. These results indicate that surface reactions involving UPD species can influence the diode properties, even

reversing the polarity under certain conditions as demonstrated here, contributing the switchable photovoltaic effect.[9]

We should give some attention to Au^0/Au$^+$ reactions. While we cannot rule out Au$^+$ or Au^{3+} formation in concentrations <0.1%, under the conditions in the presented XPS experiments (ultrahigh vacuum or UHV, X-ray irradiation, and numerous photoelectron collisions within the bulk), the results do not support a direct oxidative chemical reaction with Au as was previously proposed as a degradation path (evidenced by the absence of oxidized Au species in any of our Au 4f XPS spectra).[22] Typically, synthesis of Au perovskite phases (such as Cs$_2$Au$_2$Br$_6$) uses a pre-oxidized Au precursor or uses a well-known reaction between Au metal and triiodide salts (e.g., KI:I$_2$, methylammonium iodide:I$_2$).[20–22] We may understand the lack of Au$^+$ formation by recognizing that the abundance of iodide ions creates a weakly reducing environment (the fact that it remains a reducing environment is also illustrated by the observed reaction whereby Pb^{2+} is reduced to Pb^0). Furthermore, due to the differences in reduction potentials, Au$^+$ would immediately oxidize any Pb^0 at the interface reducing the Au.[21,43] This, of course, may not be the case for a heavily degraded perovskite film which likely becomes an oxidizer upon the loss of methylammonium and accumulation of neutral iodine species making Au-perovskite formation favorable.[22] We also believe Au oxidation to be plausible at large positive voltages above the I$^-$/I$^-_3$ reaction potential. In general, the type and extent of expected chemical reactions should be strongly influenced by the sample composition and characterization conditions.

Last, we provide electrochemical *J-V* characterization of an ITO/MAPbI$_3$/Au device (ITO = ground) that support the occurrence of interfacial reactions at low voltages in the solid-state. As shown in Fig. 6, cyclic voltammetry (CV) measurements of devices that have low leakage currents display an electrochemical current peak that emerges when the bias voltage exceeds a threshold value of <−0.5 V and >0.9 V. Threshold voltage behavior would not be expected for a purely capacitive, ionic drift/accumulation phenomenon—the charging and discharging rates should be equal and therefore should not provide a peak as is observed. Integration of this peak area gives surface concentrations of less than 10^{14} cm^{-2}, quantitatively comparable to a partial monolayer of singly charged ions (full monolayer ~5 × 10^{14} cm^{-2}), suggesting the current is due to surface reactions. The electrochemical stability window of this simple device is determined to be −0.5 V < stable window
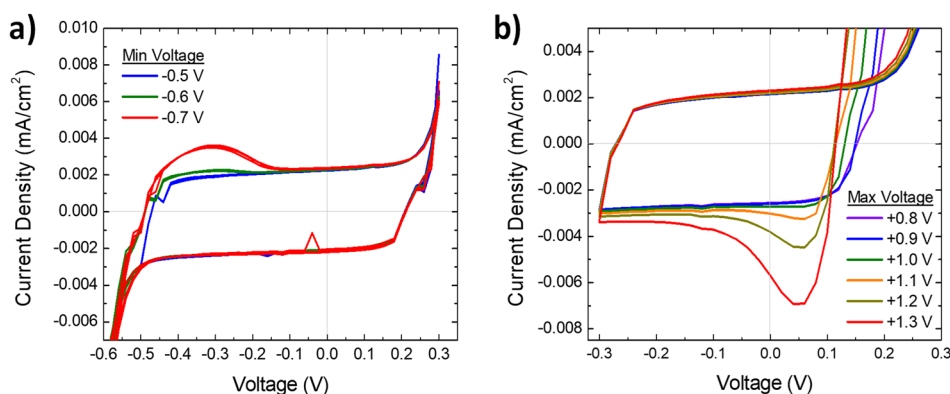

FIG. 6. Cyclic voltammetry of an ITO/MAPbI$_3$/Au device showing electrochemical peaks determining the (a) negative threshold and (b) positive threshold voltages for electrochemical reactions to occur. Measurements used a scan rate of 100 mV/s.

< 0.9 V from the threshold voltages in Figs. 6(a) and 6(b), much lower than voltages typically applied to lateral devices during characterization.[10–17] Staying within this window, the device is stable under CV characterization at 1 mV/s scan rate for >10 h (Fig. S16). By contrast, the device degrades relatively quickly when the voltage range is extended to voltages significantly more negative (−1.2 V) than the negative electrochemical threshold voltage (Fig. S17a) and to positive biases only slightly exceeding the positive threshold voltage (1.0 V, Fig. S17b). It is plausible at voltages near or above 0.9 V that I_2, I_3^-, and Au^+ formations become the dominant reaction/degradation mechanism.[17,22] Note that the voltage ranges were chosen to have comparable maximum current densities in the initial scan to ensure Joule heating effects were similar for each condition. While further investigation is needed to fully understand the degradation mechanisms of this seemingly simple device, we interpret the above results as strong indication of electrochemistry occurring at voltages well within the operating range of perovskite lateral devices, solar cells, and certainly light emitting diodes.

The diodes also displayed switchable photovoltaic properties as shown in Fig. 7. A device initially scanned from −0.6 V to +0.6 V shows Au acting as the cathode [Fig. 7(a)]. When the device is poled at positive voltages for 10 s followed by a scan to −0.6 V, the diode shows reduced photovoltaic power generation. When the poling voltage reaches +1.0 V, the diode polarity is reversed, and Au becomes the anode. A switched device to an Au anode qualitatively remains switched until the device is subjected to −0.6 V as shown by the consecutive cyclic voltage scans [Fig. 7(b)] (no voltage preconditioning). The voltage values that reverse the photovoltaic polarity correspond well to the electrochemical threshold voltages in Fig. 6 leading us to conclude that the electrochemical phenomena at these interfaces have a strong effect on photovoltaic parameters. This device architecture is known to be particularly unstable, and degradation was apparent within 1–2 h under 1 sun illumination and more rapidly at voltages near 1 V.[44]

Noble metal enhanced chemistry with halide perovskites has far reaching implications for halide perovskite devices. First, noble metals are not as inert in these systems as is commonly assumed and likely accelerate photodegradation when used as electrodes or as a substrate, especially in UHV.[5,13–16] Second, many phenomena, including current-voltage hysteresis, memristive, and switchable polarity behavior, are often broadly attributed to accumulation of mobile ions.[9,10,14] Instead, as we have previously pointed out, ion accumulation in the absence of a chemical reaction would result in ionic drift currents following basic *RC* models which is rarely the case for actual perovskite devices.[45] However, the so-called "anomalous" hysteresis and diffusion currents, which occur in various device systems ranging from photovoltaics to transistors, imply chemical reactions at interfaces.[3,9,10,45] Adsorption in the form of UPD reactions of a monolayer of iodide onto Au translates to injection of defects (vacancies) into the perovskite layer in concentrations on the order of 10^{17} cm^{-3} for a 300 nm perovskite film. Reactions will follow different mechanisms for various materials in contact with perovskites (e.g., metals, oxides, organics) giving rise to interface dependent behaviors.[46] The possibility of many different reaction mechanisms lends reasonable origin for the variety of *J-V* behaviors for seemingly similar perovskite devices. As such, the widely invoked mechanism of ion accumulation downplays the potential role of chemical reactions in the above phenomena. Finally,
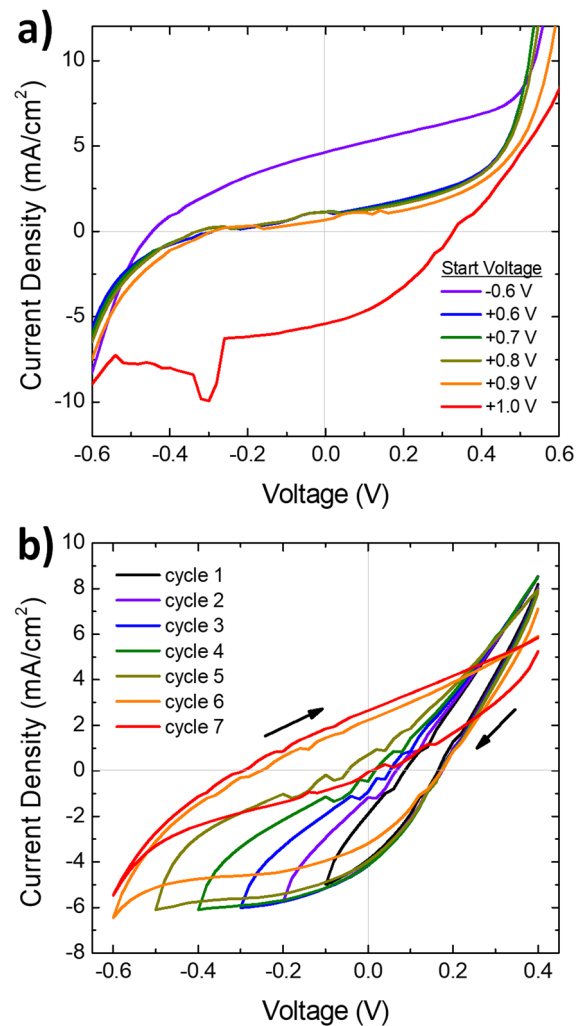

FIG. 7. (a) *J-V* scans of an ITO/MAPbI$_3$/Au device starting at different voltages showing a switch of photovoltaic polarity at +1.0 V. (b) Cyclic *J-V* of a switched device starting at +0.4 V showing polarity is not shifted back until the negative voltage reached −0.6 V. Devices were illuminated by AM1.5G simulated solar illumination.

it may be useful to adopt the concept of interphase from the electrochemical community.[29,34] Ion accumulation/depletion implies that the materials stay in the same phase and that only ion vacancies can be formed or filled. We know from the above results that the interphase can be composed of at least several atomic layers which can contain H^0_{UPD}, I^0_{UPD}, Pb_{UPD}, Pb^0, PbI_2, methylamine, methylamide, and MAPbI$_3$ in addition to the ion vacancies that are created due to the consumption of ions. The complexity of this interphase structure may influence everything from the equilibrium concentration of defects in the bulk perovskite to vacuum energy level shifts of the adsorbate "contaminated" Au surface.[47]

In summary, systematic XPS characterization of MAPbI$_3$/Au and PbI$_2$/Au interfaces reveals the formation of ionic UPD adsorbates on Au. Subtle UPD reduction/oxidation reactions may occur

for up to a monolayer of adsorbed ions forming a malleable interphase at the electrode. Changes in this interphase composition upon irradiation are capable of injecting non-negligible concentrations of defects into the perovskite bulk if ions are sufficiently mobile. More work is necessary to understand how the interphase structure and energy level alignment within devices are affected by applied voltages, other external stresses such as illumination, as well as changes across the larger chemical composition space of methylammonium containing halide perovskites. It is clear that the UPD reactions enable extrinsic reaction pathways such as liberating HI and methylamine to eventually induce Pb^0_{UPD} growth under certain characterization conditions. To probe the electrical limits of $ITO/MAPbI_3/Au$ interfaces, we conducted solid-state CV scans and determined an electrochemical stability window of -0.5 V to 0.9 V for this device. Within this window, the device can be cycled indefinitely in the dark, and J-V hysteresis behavior is linked to reversible surface reactions that alter the diode properties. Exceeding these electrochemical limits induces further reactions and rapid degradation of the device in some cases. These interesting electrochemical phenomena at perovskite/Au heterojunctions elucidate potential limitations of the use of noble metals as well as methylammonium containing perovskites for highly stable optoelectronic devices.

See supplementary material for experimental methods, tabulated XPS atomic ratios, microscopy, additional XPS spectra, and additional J-V data.

REFERENCES

[1] B. Saparov and D. B. Mitzi, "Organic–inorganic perovskites: Structural versatility for functional materials design," Chem. Rev. **116**, 4558–4596 (2016).

[2] Y. Chen, L. Zhang, Y. Zhang, H. Gao, and H. Yan, "Large-area perovskite solar cells—A review of recent progress and issues," RSC Adv. **8**, 10489–10508 (2018).

[3] Y.-H. Kim, S. Kim, S. H. Jo, and T.-W. Lee, "Metal halide perovskites: From crystal formations to light-emitting-diode applications," Small Methods **2**, 1800093 (2018).

[4] K. Wang, S. Wang, S. Xiao, and Q. Song, "Recent advances in perovskite micro- and nanolasers," Adv. Opt. Mater. **6**, 1800278 (2018).

[5] J. A. Christians, P. Schulz, J. S. Tinkham, T. H. Schloemer, S. P. Harvey, B. J. Tremolet de Villers, A. Sellinger, J. J. Berry, and J. M. Luther, "Tailored interfaces of unencapsulated perovskite solar cells for >1000 hour operational stability," Nat. Energy **3**, 68–74 (2018).

[6] J. A. Christians, S. N. Habisreutinger, J. J. Berry, and J. M. Luther, "Stability in perovskite photovoltaics: A paradigm for newfangled technologies," ACS Energy Lett. **3**, 2136–2143 (2018).

[7] B. Brunetti, C. Cavallo, A. Ciccioli, G. Gigli, and A. Latini, "On the thermal and thermodynamic (in)stability of methylammonium lead halide perovskites," Sci. Rep. **6**, 31896 (2016).

[8] A. Ciccioli and A. Latini, "Thermodynamics and the intrinsic stability of lead halide perovskites $CH_3NH_3PbX_3$," J. Phys. Chem. Lett. **9**, 3756–3765 (2018).

[9] Z. Xiao, Y. Yuan, Y. Shao, Q. Wang, Q. Dong, C. Bi, P. Sharma, A. Gruverman, and J. Huang, "Giant switchable photovoltaic effect in organometal trihalide perovskite devices," Nat. Mater. **14**, 193–198 (2015).

[10] J. Choi, J. S. Han, K. Hong, S. Y. Kim, and H. W. Jang, "Organic–inorganic hybrid halide perovskites for memories, transistors, and artificial synapses," Adv. Mater. **30**, 1704002 (2018).

[11] Y. Chen, H. T. Yi, X. Wu, R. Haroldson, Y. N. Gartstein, Y. I. Rodionov, K. S. Tikhonov, A. Zakhidov, X.-Y. Zhu, and V. Podzorov, "Extended carrier lifetimes and diffusion in hybrid perovskites revealed by Hall effect and photoconductivity measurements," Nat. Commun. **7**, 12253 (2016).

[12] Q. Dong, Y. Fang, Y. Shao, P. Mulligan, J. Qiu, L. Cao, and J. Huang, "Electron-hole diffusion lengths >175 μm in solution-grown $CH_3NH_3PbI_3$ single crystals," Science **347**, 967–970 (2015).

[13] Y. Li, X. Xu, C. Wang, B. Ecker, J. Yang, J. Huang, and Y. Gao, "Light induced degradation of $CH_3NH_3PbI_3$ thin film," J. Phys. Chem. C **121**, 3904–3910 (2017).

[14] Y. Yuan, Q. Wang, Y. Shao, H. Lu, T. Li, A. Gruverman, and J. Huang, "Electric-field-driven reversible conversion between methylammonium lead triiodide perovskites and lead iodide at elevated temperatures," Adv. Energy Mater. **6**, 1501803 (2016).

[15] E. J. Juarez-Perez, L. K. Ono, M. Maeda, Y. Jiang, Z. Hawasha, and Y. Qi, "Photodecomposition and thermal decomposition in methylammonium halide lead perovskites and inferred design principles to increase photovoltaic device stability," J. Mater. Chem. A **6**, 9604–9612 (2018).

[16] Y. Luo, P. Khoram, S. Brittman, Z. Zhu, B. Lai, S. P. Ong, E. C. Garnett, and D. P. Fenning, "Direct observation of halide migration and its effect on the photoluminescence of methylammonium lead bromide perovskite single crystals," Adv. Mater. **29**, 1703451 (2017).

[17] L. A. Frolova, N. N. Dremova, and P. A. Troshin, "The chemical origin of the p-type and n-type doping effects in the hybrid methylammonium–lead iodide ($MAPbI_3$) perovskite solar cells," Chem. Commun. **51**, 14917 (2015).

[18] Z. Hawash, L. K. Ono, S. R. Raga, M. V. Lee, and Y. Qi, "Air-exposure induced dopant redistribution and energy level shifts in spin-coated spiro-MeOTAD films," Chem. Mater. **27**, 562–569 (2015).

[19] P. Schulz, "Interface design for metal halide perovskite solar cells," ACS Energy Lett. **3**, 1287–1293 (2018).

[20] H. Kitagawa, N. Kojima, and T. Nakajima, "Studies of mixed-valence states in three-dimensional halogen-bridged gold compounds, $Cs_2Au^IAu^{III}X_6$, (X = Cl, Br or I). Part 2. X-Ray photoelectron spectroscopic study," J. Chem. Soc., Dalton Trans. **0**, 3121–3125 (1991).

[21] B. J. Roman, J. Otto, C. Galik, R. Downing, and M. Sheldon, "Au exchange or Au deposition: Dual reaction pathways in Au–$CsPbBr_3$ heterostructure nanoparticles," Nano Lett. **17**, 5561–5566 (2017).

[22] N. N. Shlenskaya, N. A. Belich, M. Grätzel, E. A. Goodilin, and A. B. Tarasov, "Light-induced reactivity of gold and hybrid perovskite as a new possible degradation mechanism in perovskite solar cells," J. Mater. Chem. A **6**, 1780–1786 (2018).

[23] E. Herrero, L. J. Buller, and H. D. Abruña, "Underpotential deposition at single crystal surfaces of Au, Pt, Ag and other materials," Chem. Rev. **101**, 1897–1930 (2001).

[24] P. Hale, S. Thurgate, and P. Wilkie, "Lead underpotential deposition on Au(110)," Surf. Interface Anal. **35**, 842–851 (2003).

[25] E. Gileadi, *Physical Electrochemistry: Fundamentals, Techniques, and Applications* (Wiley-VCH, Weinheim, 2011).

[26] J. F. Rodriguez and M. P. Soriaga, "Reductive desorption of iodine chemisorbed on smooth polycrystalline gold electrodes," J. Electrochem. Soc. **135**, 616–618 (1988).

[27] T. Mebrahtu, J. F. Rodriguez, B. G. Bravo, and M. P. Soriaga, "Hydrogenative/cathodic stripping of iodine chemisorbed on smooth polycrystalline platinum electrodes," J. Electroanal. Chem. **219**, 327–333 (1987).

[28]S. Ferro and A. De Battisti, "The bromine electrode. Part I: Adsorption phenomena at polycrystalline platinum electrodes," J. Appl. Electrochem. **34**, 981–987 (2004).

[29]R. D. Armstrong, "The metal-solid electrolyte interphase," J. Electroanal. Chem. **52**, 413–419 (1974).

[30]X. Zeng and S. Bruckenstein, "Underpotential deposition and adsorption of lead on gold polycrystalline electrodes: I. XPS and TOF-SIMS investigations in 0.1M NaCl electrolytes," J. Electrochem. Soc. **146**, 2549–2554 (1999).

[31]B. G. Bravo, S. L. Michelhaugh, and M. P. Soriaga, "Anodic underpotential deposition and cathodic stripping of iodine at polycrystalline and single-crystal gold. Studies by LEED, AES, XPS, and electrochemistry," J. Phys. Chem. **95**, 5245–5249 (1991).

[32]M. L. Agiorgousis, Y.-Y. Sun, H. Zeng, and S. Zhang, "Strong covalency-induced recombination centers in perovskite solar cell material $CH_3NH_3PbI_3$," J. Am. Chem. Soc. **136**, 14570–14575 (2014).

[33]J. F. Rodriguez, J. E. Harris, M. E. Bothwell, T. Mebrahtu, and M. P. Soriaga, "Surface coordination chemistry of noble-metal electrocatalysts: Oxidative addition and reductive elimination of iodide at iridium, platinum, and gold in aqueous solutions," Inorg. Chim. Acta **148**, 123–131 (1988).

[34]E. Peled and S. Menkin, "Review—SEI: Past, present and future," J. Electrochem. Soc. **164**, A1703–A1719 (2017).

[35]L. Zhao, R. A. Kerner, Z. Xiao, Y. L. Lin, K. M. Lee, J. Schwartz, and B. P. Rand, "Redox chemistry dominates the degradation and decomposition of metal halide perovskite optoelectronic devices," ACS Energy Lett. **1**, 595–602 (2016).

[36]R. A. Kerner, T. H. Schloemer, P. Schulz, J. J. Berry, J. Schwartz, A. Sellinger, and B. P. Rand, "Amine additive reactions induced by the soft Lewis acidity of Pb^{2+} in halide perovskites. Part II: Impacts of amido Pb impurities in methylammonium lead triiodide thin films," J. Mater. Chem. C (published online).

[37]Y. Guan and E. J. M. Hensen, "Ethanol dehydrogenation by gold catalysts: The effect of the gold particle size and the presence of oxygen," Appl. Catal., A **361**, 49–56 (2009).

[38]B. Zhu and R. J. Angelici, "Non-nanogold catalyzed aerobic oxidation of secondary amines to imines," Chem. Commun. **0**, 2157–2159 (2007).

[39]S. N. Habisreutinger, N. K. Noel, H. J. Snaith, and R. J. Nicholas, "Investigating the role of 4-tert butylpyridine in perovskite solar cells," Adv. Energy Mater. **7**, 1601079 (2017).

[40]W. Peng, L. Wang, B. Murali, K.-T. Ho, A. Bera, N. Cho, C.-F. Kang, V. M. Burlakov, J. Pan, L. Sinatra, C. Ma, W. Xu, D. Shi, E. Alarousu, A. Goriely, J.-H. He, O. F. Mohammed, T. Wu, and O. M. Bakr, "Solution-Grown monocrystalline hybrid perovskite films for hole-transporter-free solar cells," Adv. Mater. **28**, 3383–3390 (2016).

[41]Y.-F. Chen, Y.-T. Tsai, D. M. Bassani, R. Clerc, D. Forgács, H. J. Bolink, M. Wussler, W. Jaegermann, G. Wantz, and L. Hirsch, "Evidence of band bending induced by hole trapping at $MAPbI_3$ perovskite/metal interface," J. Mater. Chem. A **4**, 17529 (2016).

[42]E. Bandiello, J. Ávila, L. Gil-Escrig, E. Tekelenburg, M. Sessolo, and H. J. Bolink, "Influence of mobile ions on the electroluminescence characteristics of methylammonium lead iodide perovskite diodes," J. Mater. Chem. A **4**, 18614 (2016).

[43]P. Vanýsek, "Electrochemical series," in *CRC Handbook of Chemistry and Physics*, 99th ed., Internet Version, edited by J. R. Rumble (CRC Press/Taylor & Francis, Boca Raton, FL, 2018).

[44]K. Domanski, J.-P. Correa-Baena, N. Mine, M. K. Nazeeruddin, A. Abate, M. Saliba, W. Tress, A. Hagfeldt, and M. Grätzel, "Not all that glitters is gold: Metal-migration-induced degradation in perovskite solar cells," ACS Nano **10**, 6306–6314 (2016).

[45]R. A. Kerner and B. P. Rand, "Ionic–electronic ambipolar transport in metal halide perovskites: Can electronic conductivity limit ionic diffusion?," J. Phys. Chem. Lett. **9**, 132–137 (2018).

[46]I. Levine, P. K. Nayak, J. T.-W. Wang, N. Sakai, S. van Reenen, T. M. Brenner, S. Mukhopadhyay, H. J. Snaith, G. Hodes, and D. Cahen, "Interface-dependent ion migration/accumulation controls hysteresis in $MAPbI_3$ solar cells," J. Phys. Chem. C **120**, 16399–16411 (2016).

[47]F. Zhang, F. Ullrich, S. Silver, R. A. Kerner, B. P. Rand, and A. Kahn, "Complexities of contact potential difference measurements on metal halide perovskite surfaces," J. Phys. Chem. Lett. **10**, 890–896 (2019).